Journal of Medicinal Chemistry

pubs.acs.org/jmc

Article

Pd_2Spermine as an Alternative Therapeutics for Cisplatin-Resistant Triple-Negative Breast Cancer

Tatiana J. Carneiro, Ana L. M. Batista de Carvalho, Martin Vojtek, Raquel C. Laginha, Maria Paula M. Marques, Carmen Diniz,*,⊥ and Ana M. Gil*,⊥

Cite This: J. Med. Chem. 2024, 67, 6839−6853

Read Online

ACCESS | Metrics & More | Article Recommendations | Supporting Information

ABSTRACT: Cisplatin (cDDP) resistance is a matter of concern in triple-negative breast cancer therapeutics. We measured the metabolic response of cDDP-sensitive (S) and -resistant (R) MDA-MB-231 cells to Pd_2Spermine(Spm) (a possible alternative to cDDP) compared to cDDP to investigate (i) intrinsic response/resistance mechanisms and (ii) the potential cytotoxic role of Pd_2Spm. Cell extracts were analyzed by untargeted nuclear magnetic resonance metabolomics, and cell media were analyzed for particular metabolites. CDDP-exposed S cells experienced enhanced antioxidant protection and small deviations in the tricarboxylic acid cycle (TCA), pyrimidine metabolism, and lipid oxidation (proposed cytotoxicity signature). R cells responded more strongly to cDDP, suggesting a resistance signature of activated TCA cycle, altered AMP/ADP/ATP and adenine/uracil fingerprints, and phospholipid biosynthesis (without significant antioxidant protection). Pd_2Spm impacted more markedly on R/S cell metabolisms, inducing similarities to cDDP/S cells (probably reflecting high cytotoxicity) and strong additional effects indicative of amino acid depletion, membrane degradation, energy/nucleotide adaptations, and a possible beneficial intracellular γ-aminobutyrate/glutathione-mediated antioxidant mechanism.

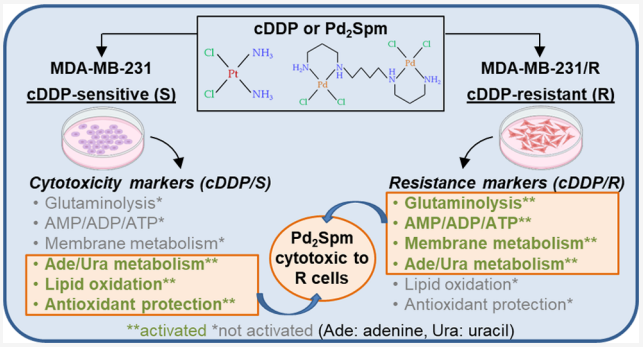

INTRODUCTION

Triple-negative breast cancer (TNBC) is a subtype of breast cancer (BC) that affects approximately 10−20% of patients and is characterized by the absence of hormone receptors (both estrogen and progesterone) and of human epidermal growth factor receptor 2.[1,2] TNBC is characterized by high metastatic potential and risk of relapse, thus leading to poor prognosis, usually associated with limited treatment options.[3,4] First-line treatments are usually based on anthracycline and taxane, whereas cytotoxic platinum(II) [Pt(II)] agents (in particular, cisplatin, cDDP) are often used in neoadjuvant therapy, increasing positive responses from about 30% up to 50%.[5] However, the efficacy of Pt(II) drugs is often hampered by toxicity and acquired resistance.[6,7] The latter (defined as tumor relapse within 6 months of initial treatment) is particularly critical in TNBC where intrinsic tumor heterogeneity is associated with increased resistance and relapse, compared to other BC subtypes.[8] These drawbacks of Pt(II)-based therapy have motivated the search for other metal-based drugs, including palladium [Pd(II)] complexes.[9−11] In particular, the Pd(II) dinuclear chelate with the biogenic polyamine spermine Pd_2Spm (Spm, $H_2N(CH_2)_3NH$-$(CH_2)_4NH(CH_2)_3NH_2$) exhibited promising *in vitro* antiproliferative, antimigratory, and antiangiogenic properties against the TNBC MDA-MB-231 cell line, along with effective responses in other cancer cell lines, e.g., leukemia, osteosarcoma, oral squamous cells, ovarian, and prostate carcinomas.[12−19] In addition, *in vivo* studies have shown a more favorable biodistribution profile of Pd(II) in healthy BALB/c mice compared to that of Pt(II), while exposure of a MDA-MB-231 cell-derived xenograft (CDX) mouse model to Pd_2Spm resulted in the reduction of tumor size and cell proliferation rate, as well as lower systemic toxicity, compared to cDDP.[20,21] Pd_2Spm also appears to be more selective for TNBC cells, having less deleterious effects on noncancerous breast cells, at least viewed under *in vitro* conditions.[21] Metabolomics has been extensively highlighted as a valuable tool towards the understanding of the interplay between drugs and cellular metabolism in breast cancer.[22] Indeed, metabolomics of CDX mice with TNBC showed that, compared to cDDP, Pd_2Spm induced (i) pronounced metabolic disturbances in tumor metabolism (energy, membrane, nucleotides, and one-carbon metabolisms), possibly reflecting a different

Received: February 21, 2024
Revised: March 25, 2024
Accepted: April 2, 2024
Published: April 9, 2024

https://doi.org/10.1021/acs.jmedchem.4c00435
J. Med. Chem. 2024, 67, 6839−6853

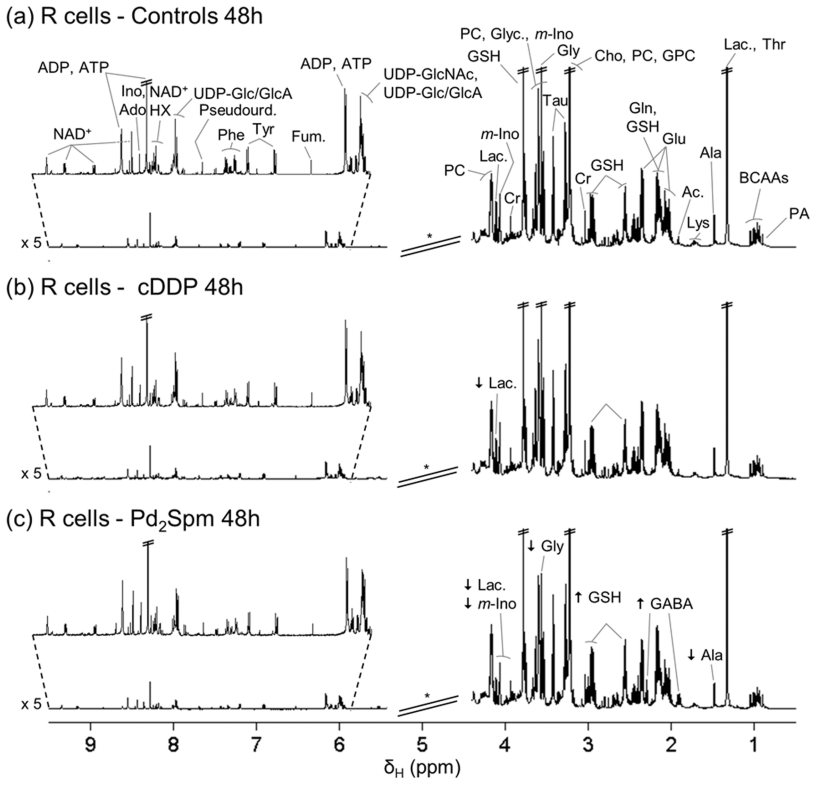

Figure 1. Average ^{1}H-NMR spectra of aqueous extracts of cDDP-resistant MDA-MB-231/R cells (48 h) (a) untreated and treated with (b) cDDP and (c) Pd_2Spm. * Cutoff of water suppression region (δ 4.4−5.4), not considered in the multivariate analysis. The arrows identify metabolic variations found with the visual inspection of spectra of treated groups in relation to controls. Abbreviations: 3-letter code for amino acids; Ac., acetate; Ado, adenosine; ADP, adenosine diphosphate; ATP, adenosine triphosphate; BCAAs, branched-chain amino acids (Ile, Leu, and Val); Cho, choline; Cr, creatine; Fum., fumarate; GABA, γ-aminobutyrate; Glyc., glycerol; GPC, glycerophosphocholine; GSH, glutathione (reduced); HX, hypoxanthine; Ino, inosine; *m*-Ino, *myo*-inositol; Lac., lactate; NAD^+, nicotinamide adenine dinucleotide (oxidized); PA, pantothenate; PC, phosphocholine; Pseudourd., pseudouridine; Tau, taurine; UDP-Glc/GlcA, uridine diphosphate-glucose/glucuronate; UDP-GlcNAc, uridine diphosphate-*N*-acetylglucosamine.

mechanism of action of the Pd(II) complex, and (ii) an enhanced neuroprotective response of brain, along with lower impact on liver.[23,24] Furthermore, Pd_2Spm administration induced initial metabolic deviations in healthy BALB/c mice, which, however, returned to control levels faster (within 48 h) than with cDDP, namely, in kidney, liver, breast tissue and brain.[25,26] This corroborated other reports of lower *in vivo* toxicity of the Pd(II) compound, compared to that of cDDP.[20,21]

In an attempt to address cDDP resistance, the biochemical effects of Pd(II) agents on cDDP-sensitive and cDDP-resistant MDA-MB-231 cells have been investigated.[27] The trinuclear chelate with spermidine (Spd, $H_2N(CH_2)_3NH(CH_2)_4NH_2$), Pd_3Sdp_2, was compared with its Pt(II)-analog Pt_3Spd_2, Pd_2Spm and cDDP. The Pd(II) complexes exhibited similar enhanced antiproliferative effects in resistant cells compared to cDDP, whereas cDDP remained the most cytotoxic agent for sensitive cells (IC_{50} after 48 h: cDDP 1 μM; Pd_2Spm 7.90 μM; Pd_3Spd_2 8.44 μM).[27] The authors suggested that the Pd(II) complexes may share a similar and effective mechanism of action against cDDP-resistant TNBC cells, probably involving other pharmacological targets besides DNA (e.g., proteins or even intracellular water).

The aim of this work was to investigate the effects of Pd_2Spm and cDDP on the metabolic profiles of cDDP-resistant (R) and cDDP-sensitive (S) MDA-MB-231 cells, measured by nuclear magnetic resonance (NMR) metabolomics. This builds upon a recently reported metabolic signature of untreated cDDP-resistant cells compared to that of sensitive cells,[28] helping to identify metabolic markers descriptive of the mechanisms of (i) resistance or sensitivity to cDDP and of (ii) the impact of Pd_2Spm, to investigate its potential to alter/treat cDDP resistance.

RESULTS

NMR Spectra of Treated cDDP-Resistant (R) and -Sensitive (S) Cells Compared to Those of Untreated Cells. The ^{1}H-NMR spectra of control (untreated) polar extracts of R cells and S cells (at 48 h) are shown in Figures 1a and S1a, respectively. Considering the spectra of R cell extracts (Figure 1), an apparent decrease is noted in lactate upon exposure to cDDP (Figure 1b) compared to controls (Figure 1a). Exposure to Pd_2Spm also seems to induce a decrease in lactate levels, although other relevant changes include increases in glutathione (GSH) and γ-aminobutyrate (GABA), among other changes (Figure 1c).

On the other hand, the NMR spectra of S cells show no clear change in lactate upon cDDP exposure (Figure S1b), although a decrease in this metabolite is again observed upon Pd_2Spm treatment (Figure S1c), together with increased GSH and GABA. Furthermore, both metal compounds appear to induce different profiles regarding amino acids and nucleotides in each cell line (Figures 1 and S1 for R and S cell lines, respectively),

https://doi.org/10.1021/acs.jmedchem.4c00435
J. Med. Chem. 2024, 67, 6839−6853

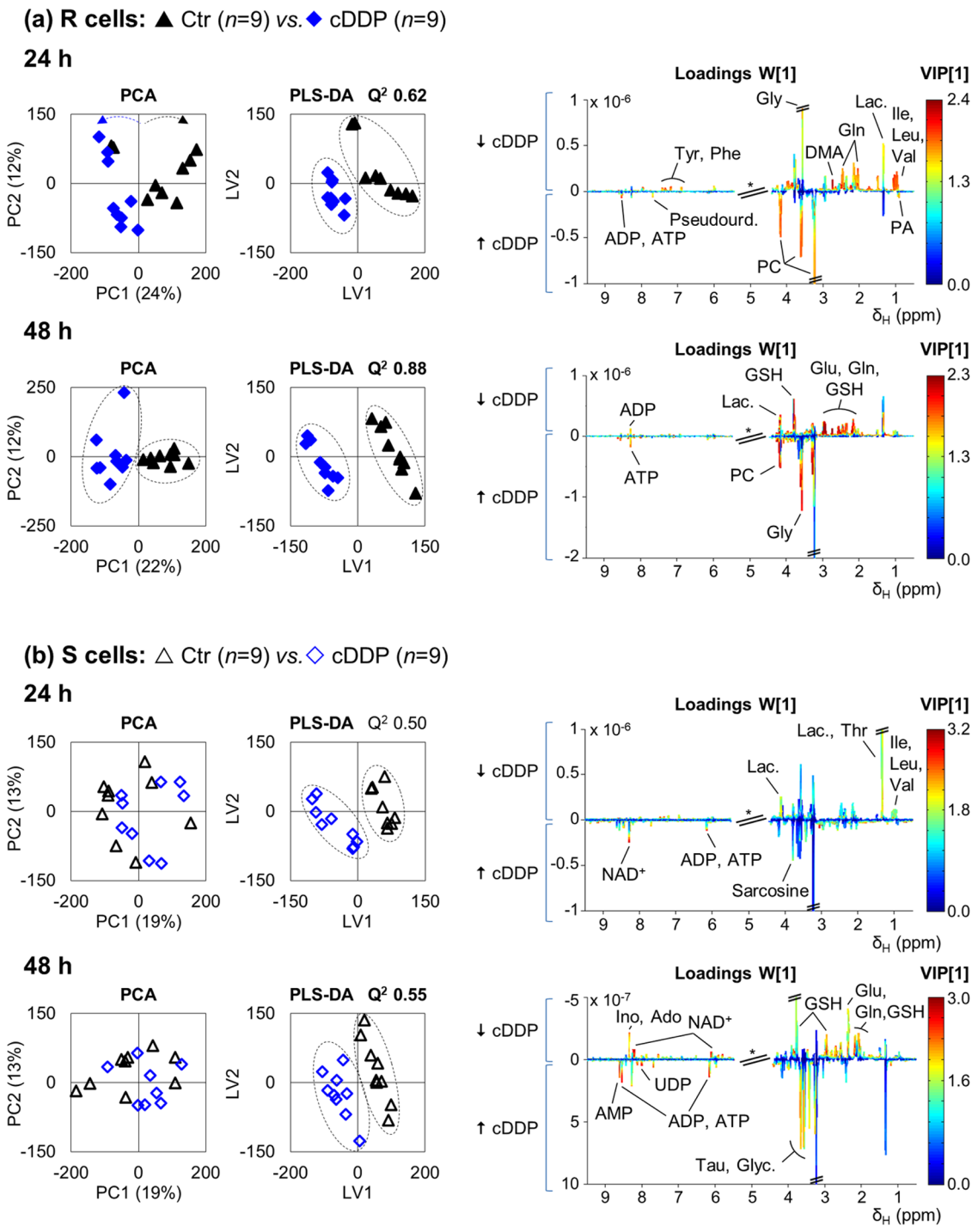

Figure 2. Pairwise PCA and PLS-DA scores and PLS-DA loading plots for ^{1}H-NMR spectra of aqueous extracts of cDDP-treated cells. (a) MDA-MB-231/R (R) and (b) MDA-MB-231 (S) cells. CDDP-treated samples (blue diamonds, $n = 9$) vs controls (black triangles, $n = 9$) at 24 and 48 h after treatment. Validation parameters (R^2 and Q^2) are shown for the PLS-DA model. Loading peak assignments are indicated for the most relevant metabolites according to VIP. Abbreviations: AMP, adenosine monophosphate; DMA, dimethylamine; UDP, uridine diphosphate; other abbreviations as defined in the caption of Figure 1.

the details of which will be further explored through statistical analysis.

Metabolic Profiling of cDDP Impact on cDDP-Resistant (R) and -Sensitive (S) Cells. PCA shows a clearer separation of controls (untreated) in cDDP-exposed R cells (Figure 2a, left) compared to S cells (Figure 2b, left). This suggests that cDDP has a stronger effect on the metabolism of R cells than on that of S cells. This observation refutes intuitive expectations that cDDP resistance would correspond to higher metabolic stability and, instead, suggests that a stronger response may reflect a possible adaptative behavior of R cell metabolism to cDDP. This result is indeed confirmed by the higher predictive power (Q^2) of the PLS-DA models obtained for R cells (Q^2 0.62 (24 h) and 0.88 (48 h); Figure 2a), compared to those obtained for S cells (Q^2 0.5 (24 h) and 0.55 (48 h); Figure 2b), as well as by the red-dominated loading

https://doi.org/10.1021/acs.jmedchem.4c00435
J. Med. Chem. 2024, 67, 6839−6853

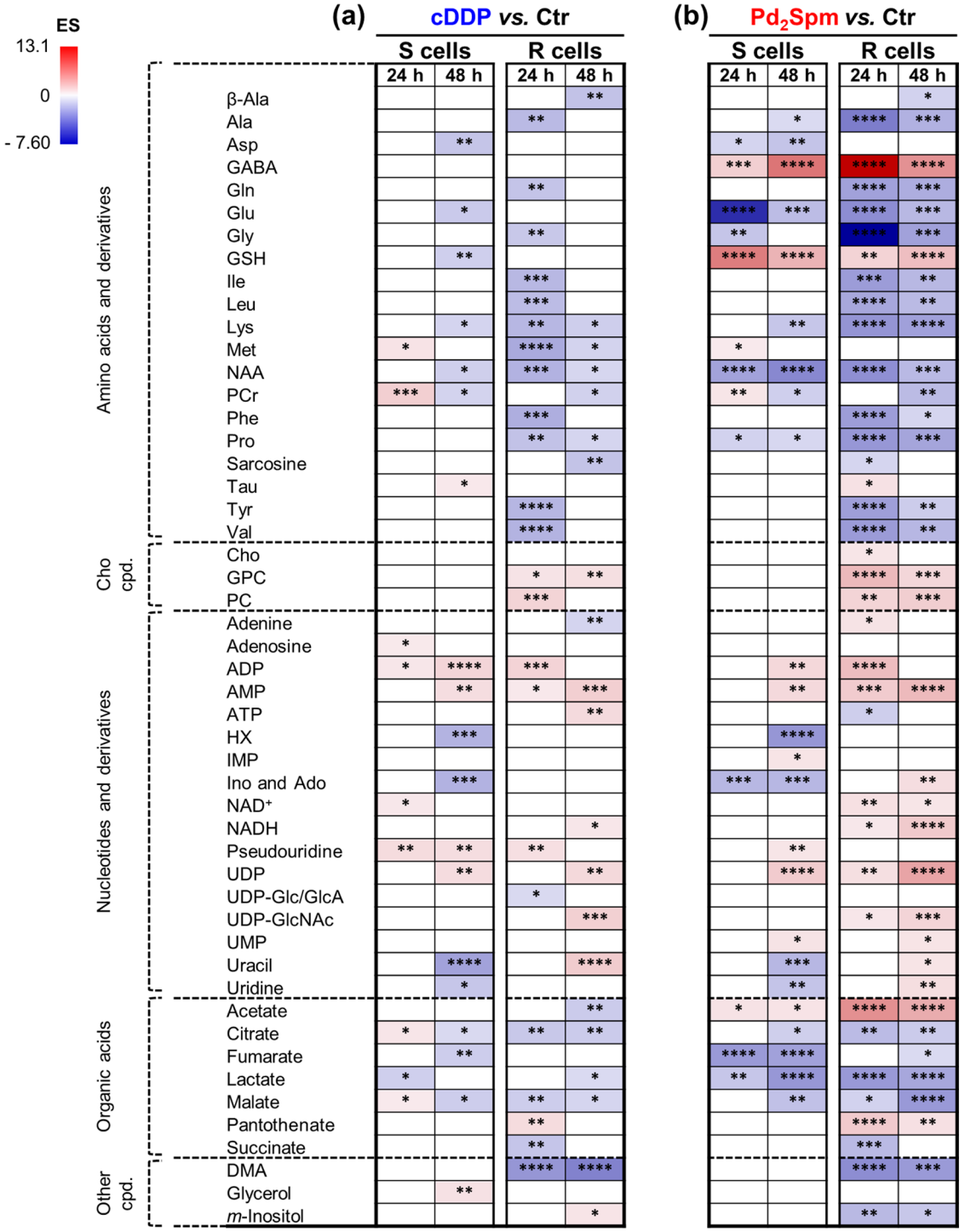

Figure 3. Heatmap of significant effect size variations for (a) cDDP-treated and (b) Pd_2Spm-treated MDA-MB-231 (S) and MDA-MB-231/R (R) cells compared to controls (untreated cells). Increasing values of effect size (ES) are colored from blue to red corresponding to negative and positive values, respectively, and are not correlated with the generic color used to designate each drug. Abbreviations: IMP, inosine monophosphate; NAA, *N*-acetyl-aspartate; NADH, nicotinamide adenine dinucleotide (reduced); PCr, phosphocreatine; UMP, uridine monophosphate; other abbreviations as defined in the captions of Figures 1 and 2. **p*-value <0.05; ***p*-value <0.01; ****p*-value <0.001; *****p*-value <0.0001 for the comparison drug *vs* controls at each time-point.

plots obtained for R cells (suggestive of larger variation; Figure 2a, right).

Indeed, clearly distinct patterns of variation are found for cDDP-exposed R cells (vs controls) compared to those for S cells (Figure 3 and Table S1). Concerning amino acids, R cells respond with an early (24 h) depletion of most amino acids, while only methionine and phosphocreatine (PCr) vary (increase) in S cells. Subsequently (48 h), many amino acids recover to control levels in R cells (blank rectangles) or to less significant decreases compared to controls. In spite of the final (48 h) amino acid pattern of R cells (relative to controls) sharing some features in common with that in S cells

https://doi.org/10.1021/acs.jmedchem.4c00435
J. Med. Chem. 2024, 67, 6839−6853

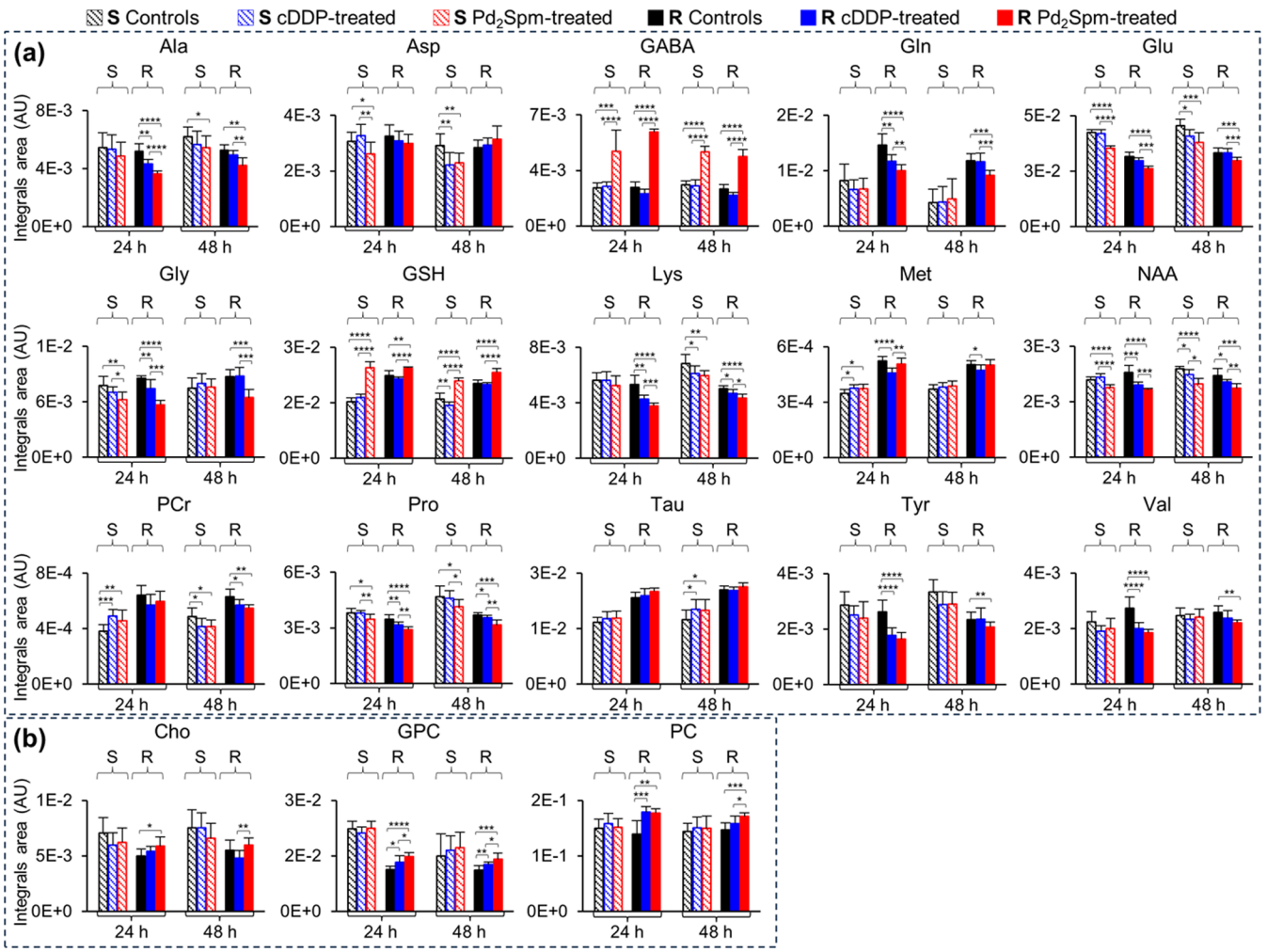

Figure 4. Time-course variations of selected (a) amino acids and (b) choline compounds in MDA-MB-231 (S, striped bars) and MDA-MB-231/R (R, full bars) cells, treated with PBS (controls, black), cDDP (blue), or Pd_2Spm (red). Values are expressed as the means of normalized peak areas ± SEM. Abbreviations are defined in the captions of Figures 1 and 3. Significant differences between treated groups (R and S cells) and controls, at each time-point: *p-value <0.05; **p-value <0.01; ***p-value <0.001; ****p-value <0.0001.

(decreased lysine, *N*-acetyl-aspartate (NAA) and PCr), it also shows clear distinctions: (i) persistent decreases in β-alanine, methionine, proline, and sarcosine (none changed in S cells at 48 h) and (ii) no increase in taurine nor decreases in aspartate, glutamate, or GSH (contrary to that observed in S cells).

The behavior of each amino acid is more clearly described in comparative plots for all groups and conditions (Figures 4a and S2 for metabolites varying more or less markedly, respectively). In these plots, the significant changes between treated and untreated samples are indicated (asterisks), whereas significant differences found in the direct comparison of S cells are listed in Table S2. Interestingly, R cells exhibit a higher glutamine/glutamate ratio than S cells under all conditions (Figure S3a), reflecting the inherently distinct glutamine and glutamate levels in R cells vs S cells (higher glutamine and lower glutamate in R cells; Figure 4a and Table S2). This ratio tends to decrease in cDDP-treated R cells (due to a decrease in glutamine) but not in S cells. Increased glycerophosphocholine (GPC) and phosphocholine (PC) appear to be a marker of R cells' response to cDDP (compared to controls), as these metabolites do not change in S cells (Figure 3a). In R cells, this is reflected by generally higher PC/choline (Cho) ratios (due to the lower Cho levels in R cells; Figure 4 and Table S2). This ratio is further increased by the cDDP treatment (Figure S3c) due to the concomitant PC increase and Cho decrease (clearer in R cells than in S cells) (Figure 4b and Table S2). For nucleotides, the pattern of variations in R cells, upon cDDP exposure, is dominated by increases, with the exception of ATP (Figure 3a and Table S1). Notably, lower nucleotide levels generally characterize both untreated[28] and cDDP-treated R cells, compared to S cells (Figures 5a and S2 and Table S2), with the exception of ATP and NADH levels (comparable between R and S). These features lead to lower ADP/ATP, AMP/ATP, and NAD^+/NADH ratios in R cells, independently of treatment (Figure S3d–f). The effect of cDDP treatment is clearer at 48 h when R cells exhibit decreased ADP/ATP and NAD^+/NADH ratios and slightly increased AMP/ATP (Figure S3d–f), while S cells only show a NAD^+/NADH decrease (Figure S3f).

Other nucleotide differences between each cDDP-treated cell line and controls (Figure 3a) include (i) decreases in hypoxanthine (HX) and inosine and/or adenosine in S cells (unchanged in R cells), (ii) marked uracil decrease and increase in S and R cells, respectively, and (iii) increased uridine diphosphate-*N*-acetylglucosamine (UDP-GlcNAc) levels in R cells (unchanged in S cells).

https://doi.org/10.1021/acs.jmedchem.4c00435
J. Med. Chem. 2024, 67, 6839−6853

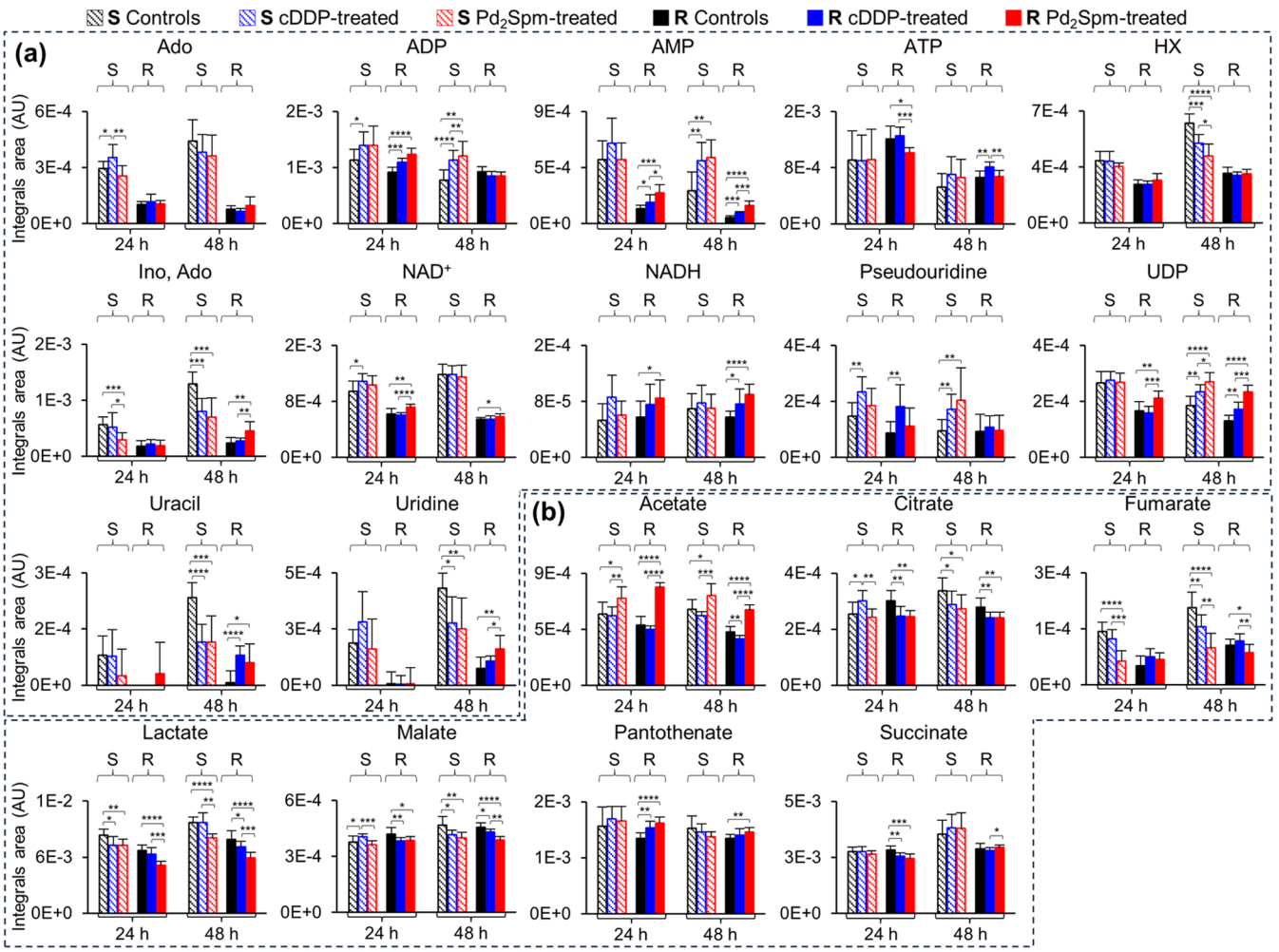

Figure 5. Time-course variations of selected (a) nucleotides and (b) organic acids in MDA-MB-231 (S, striped bars) and MDA-MB-231/R (R, full bars) cells, treated with PBS (controls, black), cDDP (blue), or Pd_2Spm (red). Values are expressed as the mean of normalized area of integrated peak ± SEM. Abbreviations are defined in the captions of Figures 1−3. Significant differences between treated groups (R and S cells) and controls, at each time-point: *p-value <0.05; **p-value <0.01; ***p-value <0.001; ****p-value <0.0001.

The two cell lines share a time-dependent depletion in the tricarboxylic acid (TCA) cycle intermediates citrate and malate, with R cells showing no change in fumarate and an additional decrease in succinate (Figure 3a and Table S1). Notably, fumarate levels are kept lower in R cells than in S cells for both controls and cDDP-treated cells (Figure 5b), whereas the remaining detectable TCA intermediates (citrate, malate, and succinate) exhibit comparable levels for both cell lines. Both cDDP-treated cell lines suffer depletion in lactate and acetate at some point during treatment (Figure 3a and Table S1), with the levels of both acids being generally kept lower for R cells, compared to S cells (Figure 5b).

In addition, R cells respond to cDDP with an increase in pantothenate (PA), whereas this compound does not change significantly in S cells (Figure 3a and Table S1). CDDP-treated R cells show a marked decrease in dimethylamine (DMA) at 24 and 48 h (absent in S cells), no increase in glycerol (noted in S cells at 48 h), and an increase in *m*-inositol at 48 h (absent in S cells) (Figures 3a and S2 and Table S1).

Metabolic Profiling of Pd_2Spm Impact on cDDP-Resistant (R) and -Sensitive (S) Cells. Multivariate analysis shows that the Pd(II) complex induces stronger metabolic responses in both R and S cells compared to cDDP, with visible PCA group separation for R cells (48 h) (Figure 6a) and S cells (24 and 48 h) (Figure 6b). PLS-DA models almost reach maximum predictive power (Q^2 1.0) for both cell lines, with a slightly higher impact of the complex on R cells (Q^2 0.91 for 24 and 48 h) compared to S cells (Q^2 0.79 and 0.81 for 24 and 48 h) (i.e., suggestive of a slightly stronger metabolic response of R cells). Compared to controls, effect size variations are indeed stronger for both Pd_2Spm-treated R and S cells (Figure 3b and Table S3), with a tendency for generally more significant changes in R cells: amino acids (dominated by decreases but including strong GSH and GABA increases in both cell lines) (Figure 4a), choline compounds (again only varying (increasing) in R cells) (Figure 4b), nucleotides (with more pronounced increases in R cells) (Figure 5a), organic acids (with more pronounced decreases in TCA cycle intermediates and increases in acetate and PA, in R cells) (Figure 5b), and decreased DMA and *m*-inositol in R cells only (Figure 5).

In relation to amino acids, increased GABA and GSH levels appear to be specific to Pd_2Spm action irrespective of cell line (Figures 3b and 4a and Table S3). Other amino acids are more strongly depleted in R cells than in S cells with no clear evidence of recuperation to control levels within 48 h (Figure 3b). Methionine remains unchanged from controls in Pd_2Spm-treated R cells (while it was strongly decreased by cDDP in the

https://doi.org/10.1021/acs.jmedchem.4c00435
J. Med. Chem. 2024, 67, 6839−6853

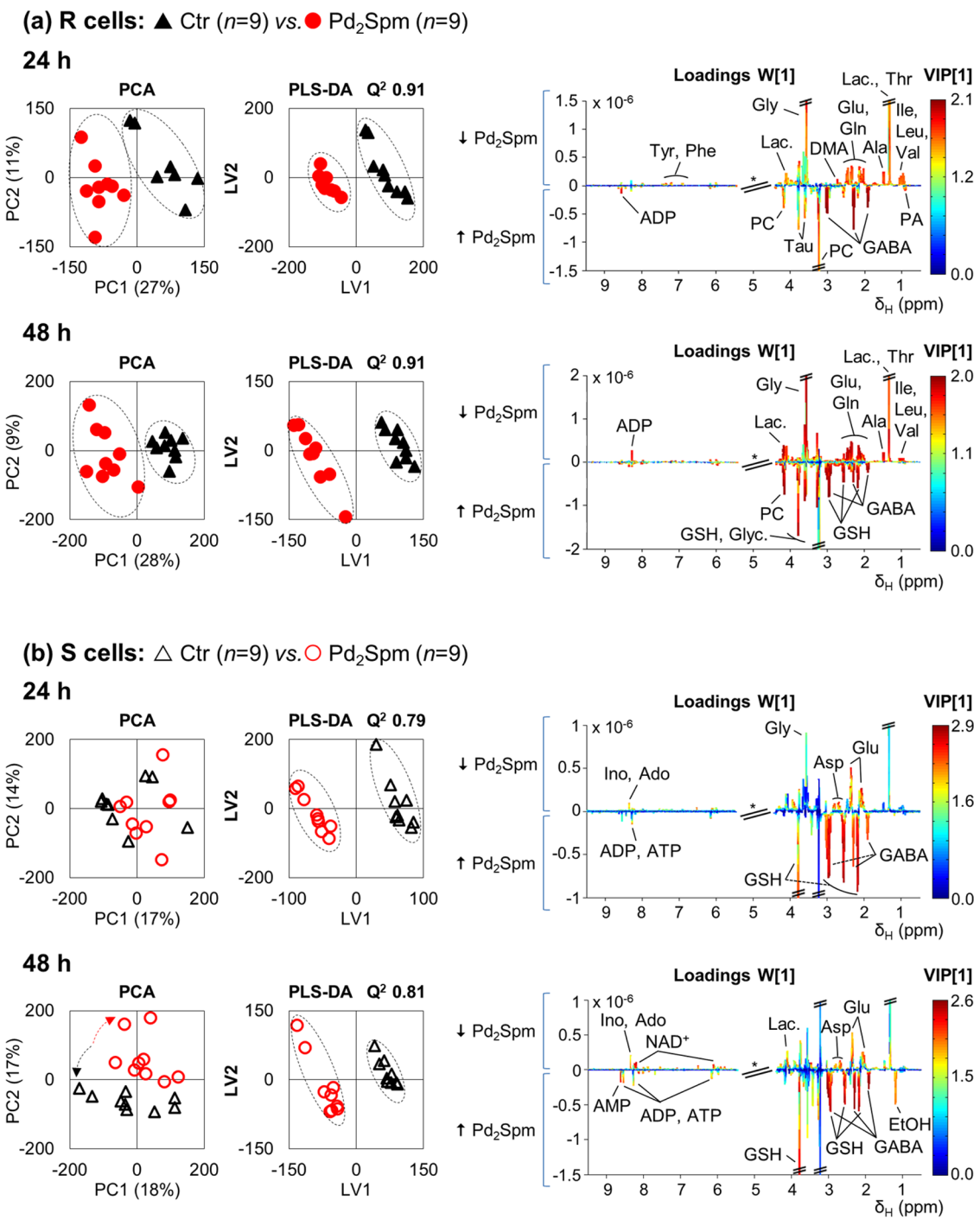

Figure 6. Pairwise PCA and PLS-DA scores and PLS-DA loading plots for ^{1}H-NMR spectra of aqueous extracts of Pd_2Spm-treated cells: (a) MDA-MB-231/R (R) and (b) MDA-MB-231 (S) cell lines. Pd_2Spm-treated samples (red circles, $n = 9$) vs controls (black triangles, $n = 9$) at 24 and 48 h after treatment. Validation parameters (R^2 and Q^2) are shown for the PLS-DA model. Loading peak assignments are indicated for the most relevant metabolites, according to VIP. Abbreviations: EtOH, ethanol; other abbreviations as defined in the captions of Figures 1 and 2.

same cells). Furthermore, Pd_2Spm action decreases the glutamine/glutamate ratio in R cells (similarly to cDDP) (Figure S3), while specifically decreasing glutamate/GABA ratio (in R and S cells) as a reflection of the important GABA increase. To test if GABA exited the cells, we examined the NMR spectra of cell media (Figure 7a,b). The GABA triplet centered at δ 2.30, which is clearly prominent in the endometabolome of Pd_2Spm-treated cells (Figure 7, left), is absent in the corresponding exometabolomes (Figure 7, right), as shown by the noncoincident superposition with the GABA profile (in orange) and the perfect coincidence with the blue outline indicating the presence of valine. Notably, although the complete absence of GABA could not be confirmed by 2D NMR due to low signal intensity, the symmetry of the valine profile rules out any significant overlap with underlying GABA peaks.

Other Pd_2Spm-induced changes include increased choline (in R cells only) (Figures 3b and 4), although treatment does not significantly change the PC/Cho ratio in either cell line, in contrast to cDDP, which was seen to increase the PC/Cho

https://doi.org/10.1021/acs.jmedchem.4c00435
J. Med. Chem. 2024, 67, 6839−6853

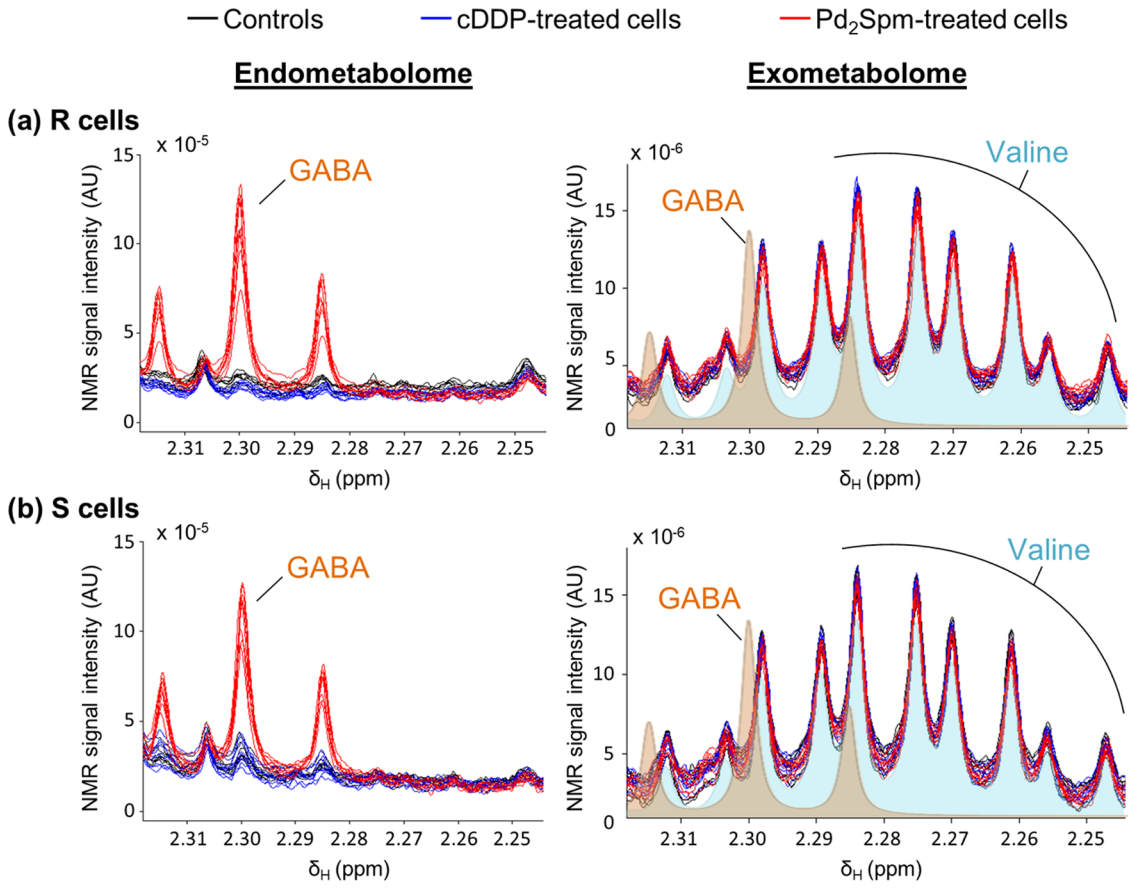

Figure 7. ^{1}H-NMR spectral regions (δ 2.24−2.32) of polar cell extracts (endometabolome, left) and cell media (exometabolome, right), illustrating intracellular GABA and its absence in extracellular media. (a) MDA-MB-231/R (R) and (b) MDA-MB-231 (S) cells treated with PBS (controls, black trace), cDDP (blue trace), or Pd_2Spm (red trace).

ratio (Figure S3). In addition, Pd_2Spm specifically induces (i) increases in adenine (R cells), IMP (S cells), inosine/adenosine (R cells), uridine monophosphate (UMP) (R and S cells), uridine (R cells), and acetate (R and S cells) and (ii) decreases in ATP and *m*-inositol (R cells) (Figures 5a and S2). In particular, nucleotide variations lead to increased ADP/ATP and AMP/ATP ratios and a decreasing trend in NAD^+/NADH (Figure S3), which is more clearly seen in Pd_2Spm-treated R cells.

DISCUSSION

cDDP Impact on MDA-MB-231 (S) and MDA-MB-231/R (R) Cell Metabolome. The cytotoxic impact of cDDP on S cells is expressed by an IC_{50} of 1.0 μM (48 h),[20] conditions under which a significant extent of cell death has been detected. Our results showed that the corresponding metabolite signature of cDDP-treated S cells includes a relatively minor disturbance of amino acid metabolism, although more enhanced at 48 h than at 24 h. At 48 h, sensitive cells are depleted in aspartate and lysine (which may be entering the TCA through oxaloacetate and acetyl-CoA, respectively) and NAA. NAA (expected to arise from *N*-acetyl-aspartyl-glutamic acid (NAAGA)) has been suggested to promote oxidative stress and lipid/protein oxidation.[29] We propose that lower NAA levels upon cDDP treatment may evidence less oxidative stress due to activated antioxidant protection mechanisms. This is consistent with an additional decrease in GSH and an increase in taurine (oxidized form of hypotaurine), suggesting the involvement of both GSH/GSSG and hypotaurine/taurine pairs, with a concomitant decrease in HX (probably through oxidation to xanthine). This protection appears to reduce the redox status of cells upon cDDP exposure, as expressed by the NAD^+/NADH decrease. This ratio is generally higher for S than for R cells, suggesting that, despite activated protective mechanisms, the former still experience higher oxidative stress, as previously proposed.[30] High glutaminolytic activity is a known feature of cancer cells,[31,32] and the globally lower glutamine/glutamate ratio (more active glutaminolysis) in S than in R cells was not affected by cDD. This suggests that the Pt(II) drug does not affect this pathway in S cells. The Pt(II) drug also does not seem to change the ATP energy status (no change in ADP/ATP and AMP/ATP), although creatine (Cr)/PCr energy metabolism is slightly disturbed. However, both ADP/ATP and AMP/ATP are kept higher (higher expenditure of ATP) in S cells, both untreated and cDDP-exposed, in relation to R cells. We hypothesize that ATP may be used more extensively in S cells to keep the membrane metabolism stable. This is consistent with the absence of changes in membrane PL precursors (namely, Cho, PC, or GPC) upon cDDP treatment of S cells.

We also postulate that ATP in S cells may be involved in pyrimidine metabolism, especially increasing pseudouridine and uridine diphosphate (UDP), at the expense of uracil and uridine. These may be related to RNA modification and enhanced glycosylation processes, respectively.[33,34] Exposure

https://doi.org/10.1021/acs.jmedchem.4c00435
J. Med. Chem. 2024, 67, 6839−6853

to cDDP slightly lowers lactate levels (at 24 h, but not at 48 h). This may reflect a preliminary shift toward less glycolytic activity and preferential use of pyruvate to feed the TCA cycle. This would support the interpretation of depletion in TCA intermediates as evidence of increased cycle activity, also supporting the anaplerotic use of aspartate and lysine mentioned above. Increased glycerol in cDDP-treated S cells may indicate some lipid oxidation, consistent with higher oxidative stress. Hence, we propose that S cells under the action of cDDP experience high oxidative stress and mobilize GSH, taurine, and HX (and, possibly, NAA) for oxidative protection and subsequent reduction of NAD^+/NADH. CDDP-treated S cells maintain the inherently high glutaminolytic activity, as well as high ADP/ATP and AMP/ATP ratios (reflecting high ATP requirements) and an effective membrane metabolism balance, as in untreated cells.[28] The high ATP consumption in the presence of cDDP (ATP probably arising through the increased TCA cycle activity and lipid oxidation) may be related to meeting the energy demands of membrane PL biosynthesis and pyrimidine metabolism.

CDDP treatment of R cells is characterized by more than one order of magnitude higher IC_{50} (32.4 μM),[27] which clearly reflects resistance of the cells to cDDP treatment. The metabolic profile of R cells is more responsive to cDDP than that of S cells, which may reflect some kind of protective behavior against the drug to avoid/reduce cell death. The early (24 h) strong demand of many amino acids, largely recovered at 48 h, may indicate an increased need for protective (antioxidative) enzymes and/or anaplerotic feeding of the TCA cycle for increased ATP production. ATP is indeed seen to increase at 48 h, as expressed by a lower ADP/ATP ratio. Glutaminolytic activity (inherently lower in R cells compared to that in S cells) is enhanced by cDDP on R cells, whereas lactate depletion also occurs (as in S cells), both observations being in agreement with enhanced TCA cycle activity. In turn, this is supported by slightly stronger depletions in citrate, malate, and succinate. Interestingly, the absence of changes in GSH, taurine, and HX suggests that no/low oxidative stress protection characterizes cDDP-treated R cells, inherently characterized by low oxidative stress. However, cDDP does induce a small NAD^+/NADH reduction (48 h), which indicates that some extent of oxidative protection is occurring but not as importantly as in S cells. Adenine is reduced in cDDP-treated R cells, probably reflecting a distinct ADP/AMP/ATP balance. Also, pyrimidine metabolism is differentially affected, suggesting a distinct glycosylation status, consistent with the increase in UDP-GlcNAc in R cells and not in S cells. Furthermore, an initial pseudouridine increase is recovered at 48 h, suggesting that R cells may have a greater capacity for RNA repair than S cells. Increased PA (vitamin B5), a precursor of CoA and of the acyl-carried protein (ACP),[35] could serve as an additional source of CoA to enhance TCA and ATP production.

However, the decrease in acetate and absence of glycerol changes (contrary to that observed in S cells) lead to the hypothesis that both PA (through ACP) and acetate may be supporting enhanced lipid biosynthesis in R cells, rather than oxidation. This is a possible sign of resistance to membrane degradation as a response to cDDP. We suggest that the enhanced anaplerotic activity of amino acids may render lipid oxidation unnecessary to attain the required higher ATP levels (and lower ADP/ATP ratio). PL metabolism responds differently in R cells, with increased PC and GPC levels (unchanged in S cells). Although this could be seen as evidence of membrane degradation, the fact that PC/Cho is consistently higher in cDDP-treated R cells may also be interpreted as a higher capacity for PL biosynthesis. This is in agreement with the supportive roles of PA and acetate suggested above, perhaps to promote cell proliferation or cell membrane repair. However, the precise origin of the choline compound profile that characterizes cDDP-treated R cells requires further investigation. Hence, cDDP treatment of R cells results in a metabolic "resistance signature" that includes significantly increased TCA cycle activity supported by amino acids (including enhanced glutaminolysis) and decreased lactate fermentation (the latter in common with cDDP-treated S cells) to increase ATP levels. In contrast with S cells, treated R cells appear to increase the level of lipid biosynthesis (possibly for PL synthesis to support cell proliferation) and exhibit a distinct pyrimidine metabolic pattern (possibly related to improved RNA repair mechanisms). Interestingly, there is no evidence of high oxidative stress (or significant protective mechanisms) in R cells (as there was in S cells), although cDDP does have a slightly lower redox status (even if this is already much lower in R cells than in S cells).

Pd_2Spm Impact on MDA-MB-231 (S) and MDA-MB-231/R (R) Cell Metabolome. The cytotoxicity of Pd_2Spm on S cells (IC_{50} 7.9 μM) is in broad agreement with that of cDDP (1.0 μM) on the same cells,[21] supporting the potential of the Pd(II) complex as a promising new drug (at least against cDDP-sensitive cells). However, a more rapid and significant response of amino acids to the Pd(II) complex (depletion of 13 anaplerotic amino acids, with no recovery at 48 h) and a stronger fumarate depletion suggest a more immediate trigger of TCA activity than in cDDP/S cells (where amino acid depletion is only seen at 48 h). Interestingly, this does not change glutamine/glutamate ratios (as also seen in cDDP/S cells). Apart from the maintenance of glutaminolytic activity, other similarities between cDDP/S cells and Pd_2Spm/S cells include no detectable changes in membrane metabolism or in ADP/ATP and AMP/ATP ratios (along with similar changes in Cr metabolism) and a number of similar nucleotide features (namely, decreased inosine/adenosine, uracil, and uridine and increased ADP, AMP, pseudouridine, UDP, and UMP). We hypothesize that the above similarities may be associated with the high cytotoxicity effects of both cDDP and Pd_2Spm on S cells (IC_{50} of 1.0 and 7.9 μM, respectively),[21] particularly regarding the above nucleotide signature. This may reflect a similar effect of cDDP/Pd_2Spm on nucleic acid damage−repair mechanisms and glycosylation processes.

With regard to the differences between Pd_2Spm and cDDP treatment on S cells, these include (i) reduced lactate production (decreased Warburg effect, as with cDDP but more effective with the Pd(II) complex, which may be considered a beneficial aspect of the latter) and (ii) slightly increased acetate (but not glycerol), suggesting some degree of lipid oxidation, although not reflected in significant changes in membrane metabolism. Redox status (NAD^+/NADH) of Pd_2Spm-treated S cells remains high and equivalent to that of untreated cells. This is contrary to cDDP, which decreased redox status slightly. Indeed, in Pd_2Spm/S cells, a different interplay of GSH/NAA seems to be involved (apparently with no involvement of taurine), and this will be further discussed below. Additionally, the absence of variation in ADP/ATP and AMP/ATP ratios found in Pd_2Spm/S cells (remaining elevated in S cells compared to that in R cells) suggests that any lipid-

https://doi.org/10.1021/acs.jmedchem.4c00435
J. Med. Chem. 2024, 67, 6839−6853

oxidation-derived ATP may be promptly consumed to maintain membrane balance and pyrimidine and inosine metabolisms. This is expressed by more enhanced levels of UMP and UDP and an increase in IMP seen only in Pd_2Spm/S cells. The increase in UMP may be related to the overexpression of uridine−cytidine kinase (CMPK1), a rate-limiting enzyme involved in the pyrimidine salvage pathway and previously associated with poor prognosis in TNBC patients.[36] However, UMP may also be in demand for phosphorylation of UDP for subsequent involvement in glycosylation processes. Thus, the exact function of enhanced UMP levels requires further investigation. The increase of IMP in Pd_2Spm/S cells, probably at the expense of inosine, may promote the activity of TCA enzymes as recently suggested,[37] contributing to the enhanced anaplerosis discussed previously. GABA and GSH increases in Pd_2Spm-treated R and S cells are clear markers of Pd_2Spm, and as this appears to be independent of cell-sensitive/resistance characteristics, it will be discussed below for both cell lines together.

The cytotoxicity of Pd_2Spm on R cells (IC_{50} 10.6 μM) is promisingly higher than that of cDDP in the same cells (32.4 μM).[27] It is noteworthy that the metabolic impact of Pd_2Spm on R cells is stronger compared to that of S cells, for instance, in terms of amino acid depletion at 24 h, with hardly any recovery of amino acid levels at 48 h (in contrast with cDDP/R cells). This may indicate that amino acid metabolism in R cells is not as resistant to Pd_2Spm as it seems to be in relation to cDDP at 48 h. In addition, as the amino acid signature of Pd_2Spm/R cells includes the changes noted in S cells as possibly indicating a positive response to treatment (namely, decreased aspartate, glutamate, lysine, NAA, and PCr and increased taurine), we postulate that such behavior in R cells treated with Pd_2Spm may reflect the higher cytotoxicity of the Pd(II) complex against R cells. The decrease in glutamine/glutamate seen for cDDP/R cells is reproduced for Pd_2Spm/R cells, with the effect thus seeming to be independent of the metal agent and a characteristic of R cells themselves. Besides the entry of amino acids into the TCA cycle, we suggest that the biosynthesis of protective proteins against enhanced oxidative stress may also occur in Pd_2Spm/R cells. This is supported by increased GSH and taurine (perhaps related to increased *m*-inositol, also reported to have antioxidant activity),[38,39] which may work to significantly reduce the NAD^+/NADH ratio, in contrast with Pd_2Spm/S cells (where such mechanism did not seem as efficient). Similarly to cDDP/R cells, increased levels of choline compounds are observed in Pd_2Spm/R cells; such a signature seems to be a general characteristic of R cells, irrespective of the treatment. However, Cho, GPC, and PC are more markedly increased upon Pd_2Spm, although no change in PC/Cho was observed (contrary to that seen in cDDP/R cells). Hence, the precise interplay of these precursors to balance PL biosynthesis and degradation of membrane lipids seems drug-dependent, and as PC/Cho is not increased by Pd_2Spm, we suggest that PL biosynthesis may not be as enhanced in Pd_2Spm/R cells as in Pd_2Spm/S cells. This supports a predominant effect of membrane degradation in Pd_2Spm/R cells, consistent with Pd_2Spm higher cytotoxicity in R cells. Indeed, the more enhanced increases in acetate and PA in Pd_2Spm/R cells are consistent with some extent of lipid oxidation, despite the lower redox status of R cells and contrary to cDDP/R cells for which we postulated a dominant role of lipid synthesis (probably of PLs).

Pd_2Spm induces further important changes in R cells, namely, additional and/or more pronounced changes in adenine and uracil derivatives, all of which increase, except for ATP. The large increases in ADP/ATP and AMP/ATP ratios are a clear characteristic of Pd_2Spm/R cells, where ATP seems to be extensively required for cell survival. Apart from the biosynthesis of antioxidant protective proteins suggested above, we hypothesize that ATP may also be supporting the altered status of nucleotide metabolism. Moreover, Pd_2Spm induces a greater depletion in lactate in R cells, implying that the Pd(II) complex is more efficient in decreasing the Warburg effect in R cells than cDDP.

Finally, marked increases in GABA (undetected in untreated and in cDDP-treated cells) and GSH (increased by Pd_2Spm and decreased by cDDP) are striking effects of Pd_2Spm on both S and R cells. Increased GABA is an issue of recognized importance in determining the prognosis of breast cancer and in particular of TNBC. Indeed, increased GABA (either of exogeneous and/or endogenous origins) triggers a complex tumor-promoting GABAergic signaling network, increasing proliferation, and metastatic potential.[40−43] It has been shown in MDA-MB-231 cells (and hence possibly in Pd_2Spm/S cells) that intracellular GABA may originate from glutamate;[42] however, glutamine/glutamate ratios are maintained in S cells. We hypothesize that a more likely origin for GABA is biogenic polyamine metabolism,[44,45] here expected to be affected by the Pd_2Spm complex itself. Indeed, the effects of both cDDP and Pd_2Spm on the expression of genes related to polyamine metabolism (including the gene spermine, spermidine N 1-acetyltransferase (SSAT)) in ovarian cancer cells[18] unveiled a distinct behavior of the palladium complex, in tandem with decreased intracellular biogenic amine levels. At this stage, the relationship of such effects with GABA levels remains unclear, although our results support the hypothesis that GABA may result from spermine carried in Pd_2Spm. In fact, intracellular spermidine and putrescine have been reported to give rise to GABA via the enzymatic action of amiloride binding protein 1 (ABP), also known as diamine oxidase (involved in the intermediate step of 4-aminobutanal formation), and aldehyde dehydrogenase 9 A1 (involved in the conversion of 4-aminobutanal in GABA).[45] The excess GABA synthesized in this pathway could then enter the TCA cycle via succinate through the action of GABA-transaminase (also known as 4-aminobutyrate aminotransferase, ABAT), although ABAT expression is known to depend on breast cancer subtype.[45,46] However, if this is the case, it does not result in a relevant succinate increase in either cell type, thus making this intracellular GABA end point insufficient to explain the impact of its marked increase. Of course, a strongly undesirable outcome would arise if GABA leaves from the intracellular medium into the extracellular matrix, where it is known to induce associated tumor-promoting properties and increased metastatic potential.[51] However, we have demonstrated that GABA is, surprisingly, retained in the intracellular environment of Pd_2Spm-treated R/S cells. Since Na^+/K^+-ATPase has been identified as an important GABA transporter, mostly studied in brain but known to be a ubiquitous transmembrane protein,[47−49] we postulate that its function in MDA-MB-231 cells may be somehow subdued in Pd_2Spm-treated cells. This ATPase pumps K^+ from the extracellular medium into the cells, in exchange for the extrusion of Na^+, while hydrolyzing intracellular ATP.[47] ATP availability is, therefore, a determinant for the adequate function of this controlled translocation

https://doi.org/10.1021/acs.jmedchem.4c00435
J. Med. Chem. 2024, 67, 6839−6853

of sodium and potassium ions across the cell membrane. We recall that in Pd_2Spm/S cells, ADP/ATP and AMP/ATP ratios remain higher than in Pd_2Spm/R cells, reflecting lower availability of ATP (due to its possible engagement in sustaining membrane balance, pyrimidine metabolism, and inosine metabolism). In addition, in Pd_2Spm/R cells, large increases in ADP/ATP and AMP/ATP ratios upon treatment indicate higher ATP requirements relative to untreated cells (suggested above to involve the biosynthesis of antioxidant protective proteins and altered status of nucleotide metabolism). Thus, we hypothesize that the use of ATP toward other ends (in S cells generally and in R cells particularly under Pd_2Spm treatment) might render ATP levels too low for the adequate function of Na^+/K^+-ATPase. The question remains as to the possible end points of the excess intracellular GABA in Pd_2Spm-treated cells. It is possible that GABA transamination will occur through ABAT to yield succinil-semialdehyde (SSA), along with alanine or glutamate (depending on the nature of the active substrate: pyruvate or α-ketoglutarate, respectively), all of these metabolites being able to enter the TCA cycle.[45] However, there is interesting recent evidence that increased GABA levels are associated with antioxidant mechanisms in a wide range of organisms.[50,51] This is indeed consistent with the concomitant marked increases in GSH, along with GABA, in all Pd_2Spm-treated cells as well as with the more marked depletion in NAA (lower NAA levels suggested earlier to evidence less oxidative stress due to activated oxidative stress protection mechanisms). We suggest that simultaneously high GSH and low NAA levels may indicate a more efficient protective mechanism in Pd_2Spm-exposed cells (with or without the involvement of taurine or HX, as these are not always seen to change), probably related to the high and comparable cytotoxicity of Pd_2Spm in both S (IC_{50} = 7.9 μM) and R cells (IC_{50} = 10.6 μM). We therefore advance the hypothesis that the Pd_2Spm-mediated increase in intracellular GABA may actually translate into a beneficial antioxidant effect, the exact mechanism of which necessarily requires further important investigation.

CONCLUSIONS

This work investigated the metabolic response of cDDP-sensitive (S) and -resistant (R) MDA-MB-231 cell lines to exposure to cDDP itself (establishing signatures of response and resistance) and to Pd_2Spm (unveiling metabolic deviations probably associated with its high cytotoxicity against both cell lines). Exposure of S cells to cDDP led to enhanced antioxidant protective mechanisms, able to decrease the inherently high redox status (NAD^+/NADH) of S cells, compared to R cells (while inherent higher glutaminolytic activity and ADP/ATP and AMP/ATP ratios were not affected). Slight deviations were induced in the TCA cycle activity (enhanced), pyrimidine metabolism, and lipid oxidation (enhanced) while leaving membrane metabolic profile unaffected. Conversely, R cell metabolism responded strongly to cDDP, supporting a proposed "resistance signature", which comprised further activated TCA cycle (amino acid/lactate depletion and activated glutaminolysis), adapted AMP/ADP/ATP status, enhanced PL biosynthesis (probably for cell proliferation and/or cell membrane repair), deviant adenine/uracil fingerprints, and, interestingly, no evidence of effective oxidative stress protection. Hence, cDDP *in vitro* resistance of MDA-MB-231 cells seems to involve larger metabolic plasticity impacting on TCA cycle activity, AMP/ADP/ATP pools, lipid and membrane metabolisms, and adenine/uracil metabolism (without significant oxidative stress effects).

Pd_2Spm impacted the metabolism of both R and S MDA-MB-231 cells more markedly than cDDP. Similarities between Pd_2Spm/S cells and cDDP/S cells (no changes in glutaminolytic activity, membrane metabolism, and AMP/ADP/ATP pools, and similar adenine/uracil derivatives patterns) are putatively associated with high cDDP/Pd_2Spm cytotoxicity upon S cells. However, marked differences arose in Pd_2Spm/S cells, including a more immediate TCA activity trigger, distinct uracil/inosine metabolisms, and prominent increases in GABA and GSH (common to Pd_2Spm/R cells). The impact of Pd_2Spm on R cells was more extensive (enhanced TCA activity, changed AMP/ADP/ATP pools, apparent membrane degradation, and altered nucleotide profile), also including features observed in cDDP/S cells as possible indicators of high cytotoxicity.

The above results suggest Pd_2Spm as effectively triggering metabolic effects possibly associated with higher cytotoxicity in S cells and, more importantly, in resistant MDA-MB-231 cells. However, Pd_2Spm also gave rise to high levels of intracellular GABA, generally known to play several undesirable roles in the cancer microenvironment once it exits cancer cells. In treated R/S cells, however, GABA did not exit the cells (perhaps due to ATP unavailability for the adequate function of Na^+/K^+-ATPase) and we hypothesize that the excess intracellular GABA may exert a beneficial antioxidant function, also involving GSH and NAA. Overall, these results illustrate the usefulness of untargeted NMR metabolomics in contributing to the understanding of cDDP sensitivity and resistance in MDA-MB-231 cells and of why Pd_2Spm may be a possible alternative to treat cDDP-resistant TNBC.

EXPERIMENTAL SECTION

Chemicals and Solutions. CDDP (*cis*-dichlorodiammine platinum(II), 99.9%), potassium tetrachloropalladate (II) (K_2PdCl_4, 98%), spermine (*N,N'*-bis(3-aminopropyl)-1,4-diaminobutane, 99%), Dulbecco's modified Eagle's medium—high-glucose cell growth medium (DMEM-HG), trypan blue (0.4% w/v), and trypsin-EDTA (1×), as well as inorganic salts and acids were all purchased from Sigma-Aldrich Chemical S.A. (Sintra, Portugal). Fetal bovine serum (FBS) was obtained from Gibco-Life Technologies (Porto, Portugal). The Pd_2Spm complex was synthesized according to published procedures.[52,53] The newly synthesized compound was characterized (and tested for purity) by ^1H NMR and Fourier transform infrared (FTIR) spectroscopy. The drugs' solutions were freshly prepared by dissolving an appropriate quantity of drug in phosphate-buffered saline, PBS (H_2PO_4 1.5 mM, Na_2HPO_4 4.3 mM, KCl 2.7 mM, NaCl 150 mM, pH 7.4). Stock solutions of cDDP (10 μM) and Pd_2Spm (79 μM) were prepared, sterile-filtered (ø 0.22 μm), and stored at −20 °C. All reagents/products were of analytical grade, and when available for purchase, they were >95% pure by HPLC analysis.

Cell Culture. The human TNBC cell line MDA-MB-231 (ATCC HTB-26; absence of estrogen and progesterone receptors, HER2 overexpression) was purchased from ATCC (Manassas, VA). MDA-MB-231 cells were cultured in DMEM-HG cell growth medium supplemented with 10% (v/v) FBS and maintained under a humidified atmosphere of 5% CO_2 at 37 °C. The cDDP-resistant cell line was established as previously described (exposure of MDA-MB-231 cells to increasing concentrations of cDDP, up to a maximum of 2 μM, during 6 months), and it was designated as MDA-MB-231/R.[27] Cell population doubling times were 25.5 ± 0.9 and 30.6 ± 1.1 h for MDA-MB-231 and MDA-MB-231/R cells, respectively. Cell cultures were routinely screened for mycoplasma contamination, with all assays having yielded negative results.

https://doi.org/10.1021/acs.jmedchem.4c00435
J. Med. Chem. 2024, 67, 6839−6853

Cell Exposure and Collection. MDA-MB-231 parental (cDDP-sensitive, S) and resistant (R) cells were seeded at a density of 3×10^4 cells/cm^2 onto 150 mm Petri dishes, cultured in a humidified atmosphere of 5% CO_2 at 37 °C, and allowed to adhere for 24 h. After this time, the experiment was initiated by adding stock solutions of each drug to achieve the corresponding half of maximal inhibitory effect IC_{50} values, previously determined for S cells: 1.0 μM cDDP and 7.9 μM Pd_2Spm.[21] The cells were then incubated and collected at 24 and 48 h, with a basis on the population doubling times mentioned above. At each time-point, cells were harvested using a 0.25% (v/v) trypsin-EDTA solution (1×), washed with PBS, and centrifuged (300*g*, 5 min, 20 °C) twice. The cell pellet was immediately stored at −80 °C until analysis. In addition, cell media were also collected at each time-point subsequently following a protein-precipitation treatment, before NMR analysis of selected metabolites.[54] Three independent experiments with triplicate were performed for each cell line, giving a total of $n = 9$ for each condition (Figure S4).

Cell Extraction. Cellular polar extracts were obtained using a methanol/chloroform/water biphasic extraction method.[55] Briefly, cell pellets were resuspended in 650 μL of 80% (v/v) methanol-MilliQ water solution, transferred to microcentrifuge tubes with 150 mg of glass beads (ø = 0.5 mm), and vortexed for 5 min to aid cell disruption. Subsequently, (i) 260 μL of 100% chloroform and (ii) 260 μL of 100% chloroform plus 220 μL MilliQ water were added to samples, which were then vortexed for 5 min between solvent addition. Samples were stored at −20 °C for 10 min and centrifuged (2000*g*, 15 min, room temperature). The aqueous phase was collected into a new tube, vacuum-dried, and stored at −80 °C until further analysis. All samples and reagents were kept on ice during the extraction procedure. Before NMR analysis, the dry aqueous extracts were suspended in 650 μL of 100 mM sodium phosphate buffer (pH 7.4, in D_2O containing 0.25% 3-(trimethylsilyl)-propionic-2,2,3,3-d4 acid (TSP) for chemical shift referencing) and transferred into 5 mm NMR tubes.

NMR Spectroscopy and Statistical Analysis of Spectra. The NMR spectra were recorded at 298 K on a Bruker AVANCE III spectrometer equipped with a 5 mm TXI probe, operating at 500.13 MHz for ^{1}H observation. Standard 1D ^{1}H-NMR spectra of aqueous extracts (and selected media samples) were acquired using a water presaturation pulse sequence ("noesypr1d" from Bruker library, Rheinstetten, Germany), with a 7002.801 Hz spectral width, 32 k data points, a 2.34 s acquisition time, and a 2 s relaxation delay and 512 scans. Prior to Fourier transformation, each free-induction decay was zero-filled to 64 k points and multiplied by a 0.3 Hz exponential line-broadening function. Spectra were manually preprocessed including phase correction, baseline adjustment, and internal calibration of chemical shifts to TSP. For peak assignment, 2D NMR homonuclear total correlation (TOCSY) and heteronuclear single-quantum correlation (HSQC) spectra were acquired for selected samples, along with comparison with the existing literature and spectral databases, such as Bruker BIOREFCODE (AMIX-viewer 3.9.14, Bruker Biospin, Rheinstetten, Germany), human metabolome database (HMDB),[56] and Chenomx NMR Suite (Chenomx Inc., Edmonton, AB, Canada).[56] Additionally, the assignment of selected peaks was confirmed by statistical total correlation spectroscopy (STOCSY) (Matlab 8.3.0, The MathWorks Inc., Natick, MA).[57] The 1D ^{1}H NMR spectra were converted into matrices (AMIX 3.9.14, Bruker Biospin, Rheinstetten, Germany), excluding methanol (δ 3.36, singlet) and water (δ 4.4−5.4) spectral regions. The spectra were aligned by recursive segment-wise peak alignment (RSPA) to minimize chemical shift variations (Matlab 8.3.0, The MathWorks Inc., Natick, Massachusetts) and normalized to the total spectral area to account for different cell numbers. Multivariate analysis was carried out using principal component analysis (PCA) and partial least-squares-discriminant analysis (PLS-DA), after unit variance (UV) scaling (SIMCA-P 11.5; Umetrics, Umeå, Sweden). PLS-DA models with values of predictive power (Q^2) higher than 0.50 were considered eligible for further analysis. PLS-DA loadings were back-transformed, multiplying each variable by its standard deviation and colored according to variable importance to the projection (VIP) (Matlab 8.3.0, The MathWorks Inc., Natick, MA). Loading plots revealed candidate resonances relevant for class separation, which were selected for area integration (AMIX 3.9.14, Bruker BioSpin, Rheinstetten, Germany), normalization, and variation assessment by univariate analysis. Univariate analysis of metabolites included effect size (ES) and statistical significance calculation (Shapiro−Wilk test to assess data normality, Student's t test, or Wilcoxon test for normally distributed or non-normally distributed data, respectively) (R statistical software).[58] For multiple testing, p-values of significantly changed metabolite levels ($|ES| >$ ES error and $p < 0.05$) were corrected by false discovery rate (FDR), based on the Benjamini and Hochberg method.[59] Significant metabolite differences were confirmed by visual inspection of the spectra and putatively interpreted based on the literature and the Kyoto Encyclopedia of Genes and Genomes (KEGG) database.[60]

■ ASSOCIATED CONTENT

Supporting Information

The Supporting Information is available free of charge at https://pubs.acs.org/doi/10.1021/acs.jmedchem.4c00435.

Figure S1. Average 500 MHz ^{1}H-NMR spectra of aqueous extracts of cDDP-sensitive MDA-MB-231 cells (a) untreated and treated with (b) cDDP and (c) Pd_2Spm after 48 h; Figure S2. Bar charts illustrating time-course variations of (a) amino acids, (b) nucleotides, and (c) other compounds significantly changed in MDA-MB-231 and MDA-MB-231/R cells; Figure S3. Bar charts illustrating time-course variations of ratios (a) Gln/Glu, (b) Glu/GABA, (c) PC/Cho, (d) ADP/ATP, (e) AMP/ATP, and (f) NAD^+/NADH, calculated for MDA-MB-231 and MDA-MB-231/R cells; Figure S4. Workflow illustrating the treatment protocol of triple-negative breast cancer cDDP-sensitive (MDA-MB-231) and -resistant (MDA-MB-231/R) cell lines; Table S1. Statistically significant metabolite variations observed in MDA-MB-231 cDDP-sensitive (S) and -resistant (R) cells treated with cDDP, compared to controls; Table S2. Statistically significant metabolite variations observed in MDA-MB-231/R (R) cells directly compared to MDA-MB-231 (S) cells, considering controls (left), cDDP-treated (middle), and Pd_2Spm-treated (right) groups at 48 h only; and Table S3. Statistically significant metabolite variations observed in MDA-MB-231 cDDP-sensitive (S) and -resistant (R) cells treated with Pd_2Spm, compared to controls (PDF)

■ AUTHOR INFORMATION

Corresponding Authors

Carmen Diniz − *LAQV/REQUIMTE, Laboratory of Pharmacology, Department of Drug Sciences, Faculty of Pharmacy, University of Porto, 4150-755 Porto, Portugal*; Phone: +351 220428608; Email: cdiniz@ff.up.pt

Ana M. Gil − *Department of Chemistry and CICECO − Aveiro Institute of Materials, University of Aveiro, 3810-193 Aveiro, Portugal*; orcid.org/0000-0003-3766-4364; Phone: +351 234370707; Email: agil@ua.pt

Authors

Tatiana J. Carneiro − *Department of Chemistry and CICECO − Aveiro Institute of Materials, University of Aveiro, 3810-193 Aveiro, Portugal; Molecular Physical-Chemistry R&D Unit, Department of Chemistry, University of Coimbra, 3004-535 Coimbra, Portugal; LAQV/REQUIMTE, Laboratory of Pharmacology, Department of Drug Sciences,*

https://doi.org/10.1021/acs.jmedchem.4c00435
J. Med. Chem. 2024, 67, 6839−6853

Faculty of Pharmacy, University of Porto, 4150-755 Porto, Portugal

Ana L. M. Batista de Carvalho − *Molecular Physical-Chemistry R&D Unit, Department of Chemistry, University of Coimbra, 3004-535 Coimbra, Portugal*

Martin Vojtek − *LAQV/REQUIMTE, Laboratory of Pharmacology, Department of Drug Sciences, Faculty of Pharmacy, University of Porto, 4150-755 Porto, Portugal*

Raquel C. Laginha − *Molecular Physical-Chemistry R&D Unit, Department of Chemistry, University of Coimbra, 3004-535 Coimbra, Portugal*

Maria Paula M. Marques − *Molecular Physical-Chemistry R&D Unit, Department of Chemistry, University of Coimbra, 3004-535 Coimbra, Portugal; Department of Life Sciences, Faculty of Science and Technology, University of Coimbra, 3000-456 Coimbra, Portugal;* orcid.org/0000-0002-8391-0055

Complete contact information is available at: https://pubs.acs.org/10.1021/acs.jmedchem.4c00435

Author Contributions

[⊥]A.M.G. and C.D. contributed equally to this work. A.M.G., M.P.M.M., and C.D. conceptualized the work, acquired funding sources, managed the resources, and supervised the project; T.J.C., A.M.G., C.D., M.V., A.L.M.B.C., and R.C.L. performed the experiments, data collection, formal data analysis, and validated the results; T.J.C. performed data acquisition, data analysis, and prepared all of the visual content of the manuscript; T.J.C. and A.M.G. wrote the original manuscript draft. All authors contributed to the investigation of state of the art, methodology development, writing/editing—review of the final version of the manuscript, and all authors reviewed and agreed to the published version of the manuscript.

Funding

This work was developed within the CICECO-Aveiro Institute of Materials projects UIDB/50011/2020 (10.54499/UIDB/50011/2020), UIDP/50011/2020 (10.54499/UIDP/50011/2020), and LA/P/0006/2020 (10.54499/LA/P/0006/2020), QFMUC—Molecular Physical Chemistry R&D Unit projects UIDB/00070/2020 (10.54499/UIDB/00070/2020) and UIDP/00070/2020 (10.54499/UIDP/00070/2020), LAQV/REQUIMTE—Associate Laboratory for Green Chemistry projects 10.54499/LA/P/0008/2020, 10.54499/UIDP/50006/2020, and 10.54499/UIDB/50006/2020, and the A.L.M.B.C. employment contract (10.54499/CEECIND/00069/2017/CP1460/CT0029) financed by national funds through the Portuguese Foundation for Science and Technology (FCT). The authors are grateful to the Portuguese National NMR Network (PTNMR), supported by FCT funds as the NMR spectrometer used is part of PTNMR and partially supported by Infrastructure Project No. 022161 (cofinanced by FEDER through COMPETE 2020, POCI and PORL, and the FCT through PIDDAC). T.J.C. thanks FCT for her Ph.D. grant SFRH/BD/145920/2019, and M.V. thanks the FCT and the Ph.D. Program in Medicines and Pharmaceutical Innovation (i3DU) for his Ph.D. grant PD/BD/135460/2017; both grants were funded by the European Social Fund of the European Union and national FCT/MCTES funds.

Notes

The authors declare no competing financial interest.

ACKNOWLEDGMENTS

Rita Oliveira is acknowledged for her support of cell culture.

ABBREVIATIONS

Ac., acetate; ACP, acyl-carried protein; Ado, adenosine; ADP, adenosine diphosphate; AMP, adenosine monophosphate; ATP, adenosine triphosphate; BC, breast cancer; BCAAs, branched-chain amino acids; cDDP, cisplatin; CDX, cell-derived xenograft; Cho, choline; Cr, creatine; DMA, dimethylamine; ES, effect size; FBS, fetal bovine serum; FDR, false discovery rate; Fum., fumarate; GABA, γ-aminobutyrate; Glyc., glycerol; GPC, glycerophosphocholine; GSH/GSSG, glutathione (reduced/oxidized forms); HX, hypoxanthine; IMP, inosine monophosphate; Ino, inosine; *m*-Ino, *myo*-inositol; Lac., lactate; NAA, *N*-acetyl-aspartate; NAD^+/NADH, nicotinamide adenine dinucleotide (oxidized/reduced); NMR, nuclear magnetic resonance; PA, pantothenate; PBS, phosphate-buffered saline; PC, phosphocholine; PCA, principal component analysis; PCr, phosphocreatine; Pd_2Spm, palladium-spermine complex; PLs, phospholipids; PLS-DA, partial least-squares-discriminant analysis; Pseudourd., pseudouridine; Q^2, predictive power; Spd, spermidine; Spm, spermine; Tau, taurine; TCA, tricarboxylic acid cycle; TNBC, triple-negative breast cancer; UDP, uridine diphosphate; UDP-Glc/GlcA, uridine diphosphate-glucose/glucuronate; UDP-GlcNAc, uridine diphosphate-*N*-acetylglucosamine; UMP, uridine monophosphate; VIP, variable importance to the projection; FTIR, Fourier transform infrared; HMDB, human metabolome database; INS, inelastic neutron scattering; KEGG, Kyoto Encyclopedia of Genes and Genome; TSP, 3-(trimethylsilyl)-propionic-2,2,3,3-d4 acid; UV, unit variance

REFERENCES

(1) Perou, C. M.; Sørlie, T.; Eisen, M. B.; van de Rijn, M.; Jeffrey, S. S.; Rees, C. A.; Pollack, J. R.; Ross, D. T.; Johnsen, H.; Akslen, L. A.; Fluge, O.; Pergamenschikov, A.; Williams, C.; Zhu, S. X.; Lønning, P. E.; Børresen-Dale, A. L.; Brown, P. O.; Botstein, D. Molecular portraits of human breast tumours. *Nature* **2000**, *406*, 747−752.

(2) Sørlie, T.; Perou, C. M.; Tibshirani, R.; Aas, T.; Geisler, S.; Johnsen, H.; Hastie, T.; Eisen, M. B.; van de Rijn, M.; Jeffrey, S. S.; Thorsen, T.; Quist, H.; Matese, J. C.; Brown, P. O.; Botstein, D.; Lønning, P. E.; Børresen-Dale, A. L. Gene expression patterns of breast carcinomas distinguish tumor subclasses with clinical implications. *Proc. Natl. Acad. Sci. U.S.A.* **2001**, *98*, 10869−10874.

(3) Zagami, P.; Carey, L. A. Triple negative breast cancer: pitfalls and progress. *NPJ Breast Cancer* **2022**, *8*, No. 95.

(4) Li, Y.; Zhang, H.; Merkher, Y.; Chen, L.; Liu, N.; Leonov, S.; Chen, Y. Recent advances in therapeutic strategies for triple-negative breast cancer. *J. Hematol. Oncol.* **2022**, *15*, No. 121.

(5) Poggio, F.; Bruzzone, M.; Ceppi, M.; Pondé, N. F.; La Valle, G.; Del Mastro, L.; de Azambuja, E.; Lambertini, M. Platinum-based neoadjuvant chemotherapy in triple-negative breast cancer: a systematic review and meta-analysis. *Ann. Oncol.* **2018**, *29*, 1497−1508.

(6) Nedeljković, M.; Damjanović, A. Mechanisms of chemotherapy resistance in triple-negative breast cancer-how we can rise to the challenge. *Cells* **2019**, *8*, 957.

(7) Zhu, Y.; Hu, Y.; Tang, C.; Guan, X.; Zhang, W. Platinum-based systematic therapy in triple-negative breast cancer. *Biochim. Biophys. Acta Rev. Cancer.* **2022**, *1877*, No. 188678.

(8) Moore-Smith, L.; Forero-Torres, A.; Stringer-Reasor, E. Future developments in neoadjuvant therapy for triple-negative breast cancer. *Surg. Clin. North Am.* **2018**, *98*, 773−785.

(9) Domínguez-Martís, E.; Mosteiro-Miguéns, D. G.; Vigo-Gendre, L.; López-Ares, D.; Freire-Garabal, M.; Núñez-Iglesias, M. J.; Novío,

S. Non-platinum metal complexes as potential anti-triple negative breast cancer agents. *Crystals* **2018**, *8*, 369.
(10) Nayeem, N.; Contel, M. Exploring the potential of metallodrugs as chemotherapeutics for triple negative breast cancer. *Chem. - Eur. J.* **2021**, *27*, 8891−8917.
(11) Vojtek, M.; Marques, M. P. M.; Ferreira, I.M.P.L.V.O.; Mota-Filipe, H.; Diniz, C. Anticancer activity of palladium-based complexes against triple negative breast cancer. *Drug Discovery Today* **2019**, *24*, 1044−1058.
(12) Fiuza, S. M.; Holy, J.; Batista de Carvalho, L. A. E.; Marques, M. P. M. Biologic activity of a dinuclear pd(II)-spermine complex toward human breast cancer. *Chem. Biol. Drug Des.* **2011**, *77*, 477−488.
(13) Batista de Carvalho, A. L. M.; Medeiros, P. S. C.; Costa, F. M.; Ribeiro, V. P.; Sousa, J. B.; Diniz, C.; Marques, M. P. Anti-invasive and anti-proliferative synergism between docetaxel and a polynuclear pd-spermine agent. *PLoS One* **2016**, *11*, No. e0167218.
(14) Navarro-Ranninger, C.; Zamora, F.; Masaguer, J.; Perez, J.; Gonzalez, V. M.; Masaguer, J. R.; Alonso, C. Palladium(II) compounds of putrescine and spermine. Synthesis, characterization, and DNA-binding and antitumor properties. *J. Inorg. Biochem.* **1993**, *52*, 37−49.
(15) Lamego, I.; Marques, M. P. M.; Duarte, I. F.; Martins, A. S.; Oliveira, H.; Gil, A. M. Impact of the Pd_2Spermine chelate on osteosarcoma metabolism: An NMR metabolomics study. *J. Proteome Res.* **2017**, *16*, 1773−1783.
(16) Martins, A. S.; Batista de Carvalho, A. L. M.; Marques, M. P. M.; Gil, A. M. Response of osteosarcoma cell metabolism to platinum and palladium chelates as potential new drugs. *Molecules* **2021**, *26*, 4805.
(17) Soares, A.; Fiuza, S.; Goncalves, M.; de Carvalho, L. A. E. B.; Marques, M. P.; Urbano, A. M. Effect of the metal center on the antitumor activity of the analogous dinuclear spermine chelates $(PdCl_2)_2$(spermine) and $(PtCl_2)_2$(spermine). *Lett. Drug Des. Discovery* **2007**, *4*, 460−463.
(18) Tummala, R.; Diegelman, P.; Fiuza, S. M.; Batista de Carvalho, L. A.; Marques, M. P.; Kramer, D. L.; Clark, K.; Vujcic, S.; Porter, C. W.; Pendyala, L. Characterization of Pt-, Pd-spermine complexes for their effect on polyamine pathway and cisplatin resistance in A2780 ovarian carcinoma cells. *Oncol. Rep.* **2010**, *24*, 15−24.
(19) Laginha, R. C.; Martins, C. B.; Brandão, A. L. C.; Marques, J.; Marques, M. P. M.; Batista de Carvalho, L. A. E.; Santos, I. P.; Batista de Carvalho, A. L. M. Evaluation of the cytotoxic effect of Pd_2Spm against prostate cancer through vibrational microspectroscopies. *Int. J. Mol. Sci.* **2023**, *24*, 1888.
(20) Vojtek, M.; Gonçalves-Monteiro, S.; Pinto, E.; Kalivodová, S.; Almeida, A.; Marques, M. P. M.; Batista de Carvalho, A. L. M.; Martins, C. B.; Mota-Filipe, H.; Ferreira, I.M.P.L.V.O.; Diniz, C. Preclinical pharmacokinetics and biodistribution of anticancer dinuclear palladium(II)-spermine complex (Pd_2Spm) in mice. *Pharmaceuticals* **2021**, *14*, 173.
(21) Vojtek, M.; Gonçalves-Monteiro, S.; Šeminská, P.; Valová, K.; Bellón, L.; Dias-Pereira, P.; Marques, F.; Marques, M. P. M.; Batista de Carvalho, A. L. M.; Mota-Filipe, H.; Ferreira, I.M.P.L.V.O.; Diniz, C. Pd_2Spermine complex shows cancer selectivity and efficacy to inhibit growth of triple-negative breast tumors in mice. *Biomedicines* **2022**, *10*, 210.
(22) Chen, Z.; Li, Z.; Li, H.; Jiang, Y. Metabolomics: a promising diagnostic and therapeutic implement for breast cancer. *Onco. Targets Ther.* **2019**, *12*, 6797−6811.
(23) Carneiro, T. J.; Araújo, R.; Vojtek, M.; Gonçalves-Monteiro, S.; de Carvalho, A. L. M. B.; Marques, M. P. M.; Diniz, C.; Gil, A. M. Impact of the Pd_2Spm (Spermine) complex on the metabolism of triple-negative breast cancer tumors of a xenograft mouse model. *Int. J. Mol. Sci.* **2021**, *22*, No. 10775.
(24) Carneiro, T. J.; Vojtek, M.; Gonçalves-Monteiro, S.; Batista de Carvalho, A. L. M.; Marques, M. P. M.; Diniz, C.; Gil, A. M. Effect of Pd_2Spermine on mice brain-liver axis metabolism assessed by NMR metabolomics. *Int. J. Mol. Sci.* **2022**, *23*, No. 13773.
(25) Carneiro, T. J.; Araújo, R.; Vojtek, M.; Gonçalves-Monteiro, S.; Diniz, C.; Batista de Carvalho, A. L. M.; Marques, M. P. M.; Gil, A. M. Novel insights into mice multi-organ metabolism upon exposure to a potential anticancer Pd(II)-agent. *Metabolites* **2021**, *11*, 114.
(26) Carneiro, T. J.; Vojtek, M.; Gonçalves-Monteiro, S.; Neves, J. R.; Carvalho, A.L.M.B.d.; Marques, M. P. M.; Diniz, C.; Gil, A. M. Metabolic impact of anticancer drugs Pd_2Spermine and cisplatin on the brain of healthy mice. *Pharmaceutics* **2022**, *14*, 259.
(27) Vojtek, M.; Martins, C. B.; Ramos, R.; Duarte, S. G.; Ferreira, I.M.P.L.V.O.; Batista de Carvalho, A. L. M.; Marques, M. P. M.; Diniz, C. Pd(II) and Pt(II) trinuclear chelates with spermidine: selective anticancer activity towards TNBC-sensitive and -resistant to cisplatin. *Pharmaceutics* **2023**, *15*, 1205.
(28) Carneiro, T. J.; Carvalho, ALMB.; Vojtek, M.; Carmo, I. F.; Marques, M. P. M.; Diniz, C.; Gil, A. M. Disclosing a metabolic signature of cisplatin resistance in MDA-MB-231 triple-negative breast cancer cells by NMR metabolomics. *Cancer Cell Int.* **2023**, *23*, No. 310.
(29) Surendran, S.; Bhatnagar, M. Upregulation of *N*-acetylaspartic acid induces oxidative stress to contribute in disease pathophysiology. *Int. J. Neurosci.* **2011**, *121*, 305−309.
(30) Barrera, G.; Cucci, M. A.; Grattarola, M.; Dianzani, C.; Muzio, G.; Pizzimenti, S. Control of oxidative stress in cancer chemoresistance: spotlight on Nrf2 role. *Antioxidants* **2021**, *10*, 510.
(31) Sun, X.; Wang, M.; Wang, M.; Yu, X.; Guo, J.; Sun, T.; Li, X.; Yao, L.; Dong, H.; Xu, Y. Metabolic reprogramming in triple-negative breast cancer. *Front. Oncol.* **2020**, *10*, No. 428.
(32) Quek, L. E.; van Geldermalsen, M.; Guan, Y. F.; Wahi, K.; Mayoh, C.; Balaban, S.; Pang, A.; Wang, Q.; Cowley, M. J.; Brown, K. K.; Turner, N.; Hoy, A. J.; Holst, J. Glutamine addiction promotes glucose oxidation in triple-negative breast cancer. *Oncogene* **2022**, *41*, 4066−4078.
(33) Martinez, N. M.; Schaening-Burgos, C.; Gilbert, W. V. Pseudouridine site assignment by high-throughput in vitro RNA pseudouridylation and sequencing. *Methods Enzymol.* **2021**, *658*, 277−2310.
(34) Allain, E. P.; Rouleau, M.; Lévesque, E.; Guillemette, C. Emerging roles for UDP-glucuronosyltransferases in drug resistance and cancer progression. *Br. J. Cancer* **2020**, *122*, 1277−1287.
(35) Leonardi, R.; Jackowski, S. Biosynthesis of pantothenic acid and coenzyme A *EcoSal Plus* 2007, *2*, DOI: 10.1128/ecosalplus.3.6.3.4.
(36) Liu, N. Q.; De Marchi, T.; Timmermans, A.; Trapman-Jansen, A. M.; Foekens, R.; Look, M. P.; Smid, M.; van Deurzen, C. H.; Span, P. N.; Sweep, F. C.; Brask, J. B.; Timmermans-Wielenga, V.; Foekens, J. A.; Martens, J. W.; Umar, A. Prognostic significance of nuclear expression of UMP-CMP kinase in triple negative breast cancer patients. *Sci. Rep.* **2016**, *6*, No. 32027.
(37) Li, M. X.; Wu, X. T.; Jing, W. Q.; Hou, W. K.; Hu, S.; Yan, W. Inosine enhances tumor mitochondrial respiration by inducing Rag GTPases and nascent protein synthesis under nutrient starvation. *Cell Death Dis.* **2023**, *14*, 492.
(38) Bizzarri, M.; Dinicola, S.; Cucina, A. Myoinositol and inositol hexakisphosphate in the treatment of breast cancer: molecular mechanisms. In *Pre-Menopause, Menopause and Beyond*; Birkhaeuser, M.; Genazzani, A., Eds.; Springer: Cham, 2018; pp 233−241 DOI: 10.1007/978-3-319-63540-8_20.
(39) Chen, Q.; Shen, L.; Li, S. Emerging role of inositol monophosphatase in cancer. *Biomed. Pharmacother.* **2023**, *161*, No. 114442.
(40) Brzozowska, A.; Burdan, F.; Duma, D.; Solski, J.; Mazurkiewicz, M. γ-amino butyric acid (GABA) level as an overall survival risk factor in breast cancer. *Ann. Agric. Environ. Med.* **2017**, *24*, 435−439.
(41) Li, X.; Wang, H.; Yang, X.; Wang, X.; Zhao, L.; Zou, L.; Yang, Q.; Hou, Z.; Tan, J.; Zhang, H.; Nie, J.; Jiao, B. GABRP sustains the stemness of triple-negative breast cancer cells through EGFR signaling. *Cancer Lett.* **2021**, *514*, 90−102.
(42) Yang, Y.; Ren, L.; Li, W.; Zhang, Y.; Zhang, S.; Ge, B.; Yang, H.; Du, G.; Tang, B.; Wang, H.; Wang, J. GABAergic signaling as a

potential therapeutic target in cancers. *Biomed. Pharmacother.* **2023**, *161*, No. 114410.
(43) Neman, J.; Termini, J.; Wilczynski, S.; Vaidehi, N.; Choy, C.; Kowolik, C. M.; Li, H.; Hambrecht, A. C.; Roberts, E.; Jandial, R. Human breast cancer metastases to the brain display GABAergic properties in the neural niche. *Proc. Natl. Acad. Sci. U.S.A.* **2014**, *111*, 984−989.
(44) Minois, N.; Carmona-Gutierrez, D.; Madeo, F. Polyamines in aging and disease. *Aging* **2011**, *3*, 716−732.
(45) Dahn, M. L.; Walsh, H. R.; Dean, C. A.; Giacomantonio, M. A.; Fernando, W.; Murphy, J. P.; Walker, O. L.; Wasson, M. D.; Gujar, S.; Pinto, D. M.; Marcato, P. Metabolite profiling reveals a connection between aldehyde dehydrogenase 1A3 and GABA metabolism in breast cancer metastasis. *Metabolomics* **2022**, *18*, No. 9.
(46) Chen, X.; Cao, Q.; Liao, R.; Wu, X.; Xun, S.; Huang, J.; Dong, C. Loss of ABAT-mediated GABAergic system promotes basal-like breast cancer progression by activating Ca^{2+}-NFAT1 axis. *Theranostics* **2019**, *9*, 34−47.
(47) Suhail, M. Na, K-ATPase: ubiquitous multifunctional transmembrane protein and its relevance to various pathophysiological conditions. *J. Clin. Med. Res.* **2010**, *2*, 1−17.
(48) Scimemi, A. Structure, function, and plasticity of GABA transporters. *Front. Cell. Neurosci.* **2014**, *8*, No. 161.
(49) Moldavan, M.; Cravetchi, O.; Allen, C. N. GABA transporters regulate tonic and synaptic $GABA_A$ receptor-mediated currents in the suprachiasmatic nucleus neurons. *J. Neurophysiol.* **2017**, *118*, 3092−3106.
(50) Zhu, Z.; Shi, Z.; Xie, C.; Gong, W.; Hu, Z.; Peng, Y. A novel mechanism of Gamma-aminobutyric acid (GABA) protecting human umbilical vein endothelial cells (HUVECs) against H_2O_2-induced oxidative injury. *Comp. Biochem. Physiol., Part C: Toxicol. Pharmacol.* **2019**, *217*, 68−75.
(51) Ngo, D. H.; Vo, T. S. An updated review on pharmaceutical properties of gamma-aminobutyric acid. *Molecules* **2019**, *24*, 2678.
(52) Codina, G.; Caubet, A.; López, C.; Moreno, V.; Molins, E. Palladium(II) and platinum(II) polyamine complexes: x-ray crys-tal structures of (SP-4−2)-chloroN-[(3-amino-κN)propyl]propane-1,3-diamine-κN,κN′palladium(1+) tetrachloropalladate (2−) (2 :1) and (R,S)-tetrachloro[μ-(spermine)]dipalladium(II)(=μ-N,N′-bis[(3-amino-κN)propyl]butane-1,4-diamine-κN:κN′ tetrachlorodipalladium). *Helv. Chim. Acta* **1999**, *82*, 1025−1037.
(53) Fiuza, S. M.; Amado, A. M.; Parker, S. F.; Marques, M. P. M.; De Carvalho, L. A. E. B. Conformational insights and vibrational study of a promising anticancer agent: The role of the ligand in Pd(II)−amine complexes. *New J. Chem.* **2015**, *39*, 6274−6283.
(54) Bispo, D. S. C.; Michálková, L.; Correia, M.; Jesus, C. S. H.; Duarte, I. F.; Goodfellow, B. J.; Oliveira, M. B.; Mano, J. F.; Gil, A. M. Endo- and exometabolome crosstalk in mesenchymal stem cells undergoing osteogenic differentiation. *Cells* **2022**, *11*, 1257.
(55) Wu, H.; Southam, A. D.; Hines, A.; Viant, M. R. High-throughput tissue extraction protocol for NMR- and MS-based metabolomics. *Anal. Biochem.* **2008**, *372*, 204−212.
(56) Wishart, D. S.; Guo, A.; Oler, E.; Wang, F.; Anjum, A.; Peters, H.; Dizon, R.; Sayeeda, Z.; Tian, S.; Lee, B. L.; Berjanskii, M.; Mah, R.; Yamamoto, M.; Jovel, J.; Torres-Calzada, C.; Hiebert-Giesbrecht, M.; Lui, V. W.; Varshavi, D.; Varshavi, D.; Allen, D.; Arndt, D.; Khetarpal, N.; Sivakumaran, A.; Harford, K.; Sanford, S.; Yee, K.; Cao, X.; Budinski, Z.; Liigand, J.; Zhang, L.; Zheng, J.; Mandal, R.; Karu, N.; Dambrova, M.; Schiöth, H. B.; Greiner, R.; Gautam, V. HMDB 5.0: The Human Metabolome Database for 2022. *Nucleic Acids Res.* **2022**, *50*, D622−31.
(57) Cloarec, O.; Dumas, M. E.; Craig, A.; Barton, R. H.; Trygg, J.; Hudson, J.; Blancher, C.; Gauguier, D.; Lindon, J. C.; Holmes, E.; Nicholson, J. Statistical total correlation spectroscopy: an exploratory approach for latent biomarker identification from metabolic ^{1}H NMR data sets. *Anal. Chem.* **2005**, *77*, 1282−1289.
(58) Berben, L.; Sereika, S. M.; Engberg, S. Effect size estimation: Methods and examples. *Int. J. Nurs. Stud.* **2012**, *49*, 1039−1047.
(59) Benjamini, Y.; Hochberg, Y. Controlling the false discovery rate: a practical and powerful approach to multiple testing. *J. R. Stat. Soc. Ser. B* **1995**, *57*, 289−300.
(60) Kanehisa, M.; Goto, S. KEGG: Kyoto Encyclopedia of Genes and Genomes. *Nucleic Acids Res.* **2000**, *28*, 27−30.

https://doi.org/10.1021/acs.jmedchem.4c00435
J. Med. Chem. 2024, 67, 6839−6853